

# Gradient Descent Algorithm Inspired Adaptive Time Synchronization in Wireless Sensor Networks

Kasım Sinan Yıldırım, *Member, IEEE*

**Abstract**—Our motivation in this paper is to take another step forward from complex and heavyweight synchronization protocols to the easy-to-implement and lightweight synchronization protocols in WSNs. To this end, we present GraDeS, a novel multi-hop time synchronization protocol based upon gradient descent algorithm. We give details about our implementation of GraDeS and present its experimental evaluation in our testbed of MICAz sensor nodes. Our observations indicate that GraDeS is scalable, it has identical memory and processing overhead, better convergence time and comparable synchronization performance as compared to existing lightweight solutions.

**Index Terms**—Wireless Sensor Networks, Time Synchronization, Least-squares, Gradient Descent Algorithm

## I. INTRODUCTION

**R**ESOURCE constrained nodes in Wireless Sensor Networks (WSNs) are equipped with built-in hardware clocks that frequently drift apart due to their unstable low-cost crystal oscillators. Clock drift gives rise to loss of synchronization between sensor nodes which is problematic for collaborative and coordinated actions in WSNs, such as synchronous power on and shutdown of transceivers in order to reduce battery consumption. Therefore, each sensor node collects time information from its environment and constructs a software function, so-called logical clock, that represents network-wide global time. A logical clock is composed of an offset and a frequency that hold the value and speed difference between the corresponding hardware clock and the global time, respectively. The aim of time synchronization is to adjust the offsets and frequencies of the logical clocks so that estimation errors, i.e. clock skew, is minimized at any time instant.

There is an ample body of time synchronization protocols in the WSN literature, e.g. [1], [2], [3], that share the following steps to establish network-wide synchronization: (i) a reference node broadcasts its stable time information periodically; (ii) the receiver nodes adjust the offset and frequency of their logical clocks considering the received reference time; (iii) they broadcast the value of their logical clocks so that other nodes in the network synchronize by applying these steps. Least-squares regression is a common technique employed by these protocols to adjust the offsets and the frequencies of the logical clocks simultaneously [1], [2]. However, previous studies [3], [4] revealed that this technique is heavyweight in terms of processing and memory overhead, and simultaneous offset and frequency estimation gives rise to poor performance scalability. Other proposed techniques, such

as maximum likelihood estimation [5], belief propagation [6] and convex closure [7], share the drawback of having heavy processing and memory overhead that allowed these studies to present only simulation results. Hence, the practicality of these alternative techniques is quite arguable.

To overcome aforementioned problems in practice, two iterative methods are proposed [4], [8]. AVTS protocol [4] employs an efficient and adaptive search technique that adjusts the relative frequency value of the clocks by observing the sign of the clock skew. The logical clock offset is adjusted independently from its frequency by adding the observed skew to the logical clock directly. On the other hand, PISync [8] is based upon a Proportional-Integral (PI) controller and applies a proportional feedback (P) and an integral feedback (I) on the clock skew which allow to compensate offset and frequency differences, respectively. It has been reported that both iterative approaches achieve better and scalable synchronization performance with considerably less processing and memory overhead, and smaller code as compared to existing least-squares based protocols. As compared to PISync, AVTS requires knowledge about additional parameters in advance to perform its search effectively: the boundaries of the search space and the search precision affect its convergence speed and synchronization performance considerably. Hence, PISync appears to be a more promising solution in practice.

In this paper, our main contribution is to devise another iterative method to synchronize clocks in WSNs by introducing a novel time synchronization protocol, namely Gradient Descent Synchronization (GraDeS), which achieves scalable multi-hop time synchronization efficiently. In contrast to previous approaches, we formulate the frequency adjustment of the logical clocks as an optimization problem in which each sensor node is trying to find the frequency value of its logical clock that minimizes its synchronization error. Up to our knowledge of current literature, our study is the first to show that this optimization problem can be solved efficiently in practice by incorporating gradient descent algorithm [9]. We provide an extensive theoretical performance analysis of GraDeS as well as its practical implementation in TinyOS and evaluation in a testbed of 20 MICAz sensor nodes. Our theoretical and practical comparison with PISync revealed that both approaches exhibit nearly identical performances in terms of synchronization accuracy and resource overhead. As a brief conclusion, we believe that this study forms another step forward from complex and heavyweight to the easy-to-implement and lightweight time synchronization protocols in WSNs.

Kasım Sinan Yıldırım is with Embedded Software Group, TU Delft, Delft, The Netherlands (k.s.yildirim@tudelft.nl).

The remainder of this paper is organized as follows: Next section presents the system model we will use in this paper. In section III, we present pairwise GraDeS protocol, its theoretical analysis and a comparison with PISync protocol. A multi-hop synchronization approach with GraDeS is presented in section IV and section V gives details about implementation and evaluation in our testbed. Finally, section VI is the conclusion.

## II. SYSTEM MODEL

Our abstraction of a wireless sensor network is a *connected* graph  $G = (V, E)$  whose vertex set  $V = \{1, \dots, n\}$  represents the identifiers of the sensor nodes and edge set  $E \subseteq V \times V$  represents the bidirectional communication links between these nodes. Due to the *broadcast* nature of wireless communication, once a message is transmitted by any node  $u \in V$ , this message is received by all nodes  $v \in V$  such that  $\{u, v\} \in E$ . We refer these nodes, i.e. the nodes inside the communication range, as the *neighbors* of node  $u$  and denote by  $\mathcal{N}_u$ .

It is assumed sensor nodes are equipped with read-only hardware clocks subject to clock drift. At any time  $t > t_0$ , we model the hardware clock of any node  $u$  as

$$h_u(t) = h_u(t_0) + \int_{t_0}^t f_u(\sigma) d\sigma \quad (1)$$

where  $f_u(\sigma) \in [f_0 - f_{max}, f_0 + f_{max}]$  denotes the *oscillator frequency* of the hardware clock,  $f_0$  denotes the *nominal frequency* and  $\pm f_{max}$  denotes the upper and lower bounds of the *frequency deviation*. For the sake of simplicity of the analytical steps in the following sections, we model the dynamic drift of the clocks as

$$f(t) = f_0 + u(t) \quad (2)$$

such that  $u(t)$  is a uniformly distributed random variable in the interval  $[-f_{max}, f_{max}]$ .

We assume that messages are never lost during communication. For any message, the time that passes from the start of broadcast attempt until the recipient node receives it is referred as *transmission delay*. Based on central limit theory and empirical observations [10], we model the transmission delays as a Gaussian distributed random variable, denoted by  $\mathcal{T} \sim \mathcal{N}(0, \sigma_d^2)$ . The logical clock  $l_u(\cdot)$  of node  $u$  can be modeled as

$$l_u(t) = l_u(t_{up}) + \hat{\Delta}_u(t_{up})(h_u(t) - h_u(t_{up})) \quad (3)$$

where  $t_{up}$  is the latest time at which the logical clock is updated. In this model, *rate multiplier*  $\hat{\Delta}_u(t_{up})$  is the estimate of the relative frequency  $f_0/f_u(t)$  in the interval  $[t_0, t]$  and it is modified to speed-up or slow-down the logical clock. The *offset*  $l_u(t_{up})$  is used to correct the value of the logical clock with fresh time information. According this model, time synchronization can simply be considered as a distributed algorithm which updates the logical clock parameters  $l_u(t_{up})$  and  $\hat{\Delta}_u(t_{up})$  of each node  $u$  at each update time  $t_{up}$ .

## III. A NEW TIME SYNCHRONIZATION ALGORITHM FOR WIRELESS SENSOR NETWORKS: GRADES

In unconstrained optimization problems, the objective is to minimize a function  $f(x)$  where  $f : \mathbb{R}^n \rightarrow \mathbb{R}$  is convex and differentiable. It is assumed that the problem is solvable and hence there is an optimal point  $x^*$ . Since  $f$  is convex and differentiable,  $\nabla f(x^*) = 0$ . The *descent methods* produce a sequence  $x_{k+1} = x_k + \alpha_k \Delta x_k$  such that  $f(x_{k+1}) < f(x_k)$  where  $k = 0, 1, \dots$  denotes the *iteration number*,  $\alpha_k > 0$  is the *step size* and  $\Delta x_k$  is the descent direction at iteration  $k$ . Starting from an initial point  $x_0$ , a descent direction is determined and a step size is chosen at the beginning of each iteration to obtain the new sequence value. This iteration is continued until convergence. When the search direction is determined as the negative gradient  $\Delta x = -\nabla f(x)$ , the resulting algorithm is called the *gradient descent algorithm* [9]. In the following subsections, we introduce a new time synchronization protocol, namely Gradient Descent Synchronization (GraDeS), which is inspired from this algorithm.

### A. Pairwise Synchronization with GraDeS Approach

Consider pairwise time synchronization of two sensor nodes  $u$  and  $r$ , where  $r$  is the reference node which has access to the real-time  $t$ . Assume that node  $r$  transmits messages with a period of  $B$  seconds in order to inform node  $u$  about  $t$ . Let  $t_h = Bh$  for  $h = 0, 1, \dots$ , be the packet reception times of node  $u$  from node  $r$  and let  $l_r(t_h) = B.h + \mathcal{T}_h$  be the received clock where  $\mathcal{T}_h$  denotes the transmission delay at the step  $h$ . The synchronization error of node  $u$  with respect to the reference node  $r$  at any packet reception time  $t_h = Bh$  can be calculated as

$$e_u(t_h) = l_u(t_h) - l_r(t_h) - \mathcal{T}_h = l_u(t_h) - Bh - \mathcal{T}_h. \quad (4)$$

Let node  $u$  simply sets its logical clock to the received clock value to compensate the offset difference between the clocks. Formally, assume that node  $u$  applies the following correction to its logical clock

$$l_u(t_h^+) = l_u(t_h) - e_u(t_h) \quad (5)$$

where  $t_h^+$  denotes the time instant just after  $t_h$ . After this compensation, the *synchronization error*  $e_u(t_{h+1})$  at the subsequent packet reception time  $t_{h+1}$  will be mainly due to the different hardware clock frequency of the  $u$ . Applying straightforward steps, the function  $e_u(\cdot)$  can be generalized as:

$$e_u(t_{h+1}) = \hat{\Delta}_u(t_h^+) \int_{t_h^+}^{t_{h+1}} f_u(t) dt - (B + \mathcal{T}_{h+1} - \mathcal{T}_h) \quad (6)$$

where  $e_u(t_0) = 0$  and  $\hat{\Delta}_u(t_0) = 1$ .

The objective of time synchronization is to minimize the synchronization error which, in our case, is the function  $e_u(\cdot)$  of the dynamic parameter  $\hat{\Delta}_u$ . Getting inspired from the *gradient descent algorithm*, our objective reduces into finding the optimal value of  $\hat{\Delta}_u^*$  in order to minimize the squared

error function  $(e_u())^2$ . Formally, we define the steps of the GraDeS algorithm that will be employed at each updating time instant  $t_h$  as follows:

$$l_u(t_h^+) = t_h + \mathcal{T}_h, \quad (7)$$

$$\hat{\Delta}_u(t_h^+) = \hat{\Delta}_u(t_h) - \alpha \nabla e_u(t_h) \quad (8)$$

It should be noted that for all  $t \in [t_h^+, t_{h+1}^+)$  and  $\hat{\Delta}_u(t_h) = \hat{\Delta}_u(t_h^+)$ . In the update equation above,  $\nabla e_u(t_h)$  denotes the derivative of  $(e_u(t_h))^2$  with respect to  $\hat{\Delta}_u(t_h)$  at time  $t_h$ . From the equation (6), it can be observed that the function  $(e_u(t_h))^2$  is continuous and differentiable in the interval  $[t_{h-1}, t_h]$ . Therefore,

$$\nabla e_u(t_h) = 2e_u(t_h) \frac{de_u(\hat{\Delta}_u)}{d\hat{\Delta}_u}. \quad (9)$$

### B. Approximation of the Error Derivative

The derivative of  $\frac{de_u(\hat{\Delta}_u)}{d\hat{\Delta}_u}$  in the interval  $[t_h, t_{h+1}]$  can be approximated with the following equation:

$$\begin{aligned} \frac{de_u(\hat{\Delta}_u)}{d\hat{\Delta}_u} &= \frac{d\left(\hat{\Delta}_u \int_{t_h^+}^{t_{h+1}^+} f_u(t) dt - (B + \mathcal{T}_{h+1} - \mathcal{T}_h)\right)}{d\hat{\Delta}_u} \\ &= \int_{t_h^+}^{t_{h+1}^+} f_u(t) dt. \end{aligned} \quad (10)$$

We have  $E\left[\int_{t_h^+}^{t_{h+1}^+} f_u(t) dt\right] = Bf_0$  due to the fact that the frequency drift of the clocks are modeled as uniform random variables in Section (II). Therefore, the derivative becomes  $\frac{de_u(t_h)}{d\hat{\Delta}_u} = Bf_0$  in expectation. Finally, we get

$$\nabla e_u(t_h) = 2Bf_0 e_u(t_h). \quad (11)$$

### C. Proof of Convergence and Steady-State Error

With an abuse of notation, let us denote  $e(t_{h+1})$  by  $e(h+1)$  and  $\hat{\Delta}_u(t_{h+1})$  by  $\hat{\Delta}_u(h+1)$ . Based upon the update equations of GraDeS algorithm, the system evolution can be described with the following matrix equation:

$$\underbrace{\begin{bmatrix} e(h+1) \\ \hat{\Delta}_u(h+1) \end{bmatrix}}_{X(h+1)} = \begin{bmatrix} 0 & \int_{t_h^+}^{t_{h+1}^+} f_u(t) dt \\ 0 & 1 - 2\alpha B f_0 \int_{t_h^+}^{t_{h+1}^+} f_u(t) dt \end{bmatrix} \underbrace{\begin{bmatrix} e(h) \\ \hat{\Delta}_u(h) \end{bmatrix}}_{X(h)} + (B + \mathcal{T}_{h+1} - \mathcal{T}_h) \begin{bmatrix} -1 \\ 2\alpha B f_0 \end{bmatrix}. \quad (12)$$

Taking the expectation of both sides yields:

$$E[X(h+1)] = \underbrace{\begin{bmatrix} 0 & Bf_0 \\ 0 & 1 - 2\alpha B^2 f_0^2 \end{bmatrix}}_A E[X(h)] + \begin{bmatrix} -B \\ 2\alpha B^2 f_0 \end{bmatrix}. \quad (13)$$

The eigenvalues of the matrix  $A$  can be calculated by solving the determinant equation  $|A - \lambda I| = 0$ . The solution of this

equation can be obtained by solving the following quadratic equation

$$\lambda(1 - 2\alpha B^2 f_0^2 - \lambda) = 0 \quad (14)$$

whose roots are:

$$\lambda_1 = 0, \lambda_2 = 1 - 2\alpha B^2 f_0^2. \quad (15)$$

Matrix  $A$  is asymptotically stable, i.e. asymptotic convergence is established, if and only if  $|\lambda_{1,2}| < 1$ . Therefore, choosing the step size by considering the inequality below

$$0 < \alpha < \frac{1}{B^2 f_0^2} \quad (16)$$

will lead the system to converge to the asymptotically stable equilibrium point

$$\left[ \lim_{h \rightarrow \infty} E[e(h)], \lim_{h \rightarrow \infty} E[\hat{\Delta}_u(h)] \right]^T = [e(\infty), \hat{\Delta}_u(\infty)]^T \quad (17)$$

Therefore

$$\hat{\Delta}_u(\infty) = (1 - 2\alpha B^2 f_0^2) \hat{\Delta}_u(\infty) + 2\alpha B^2 f_0,$$

which indicates that

$$\hat{\Delta}_u(\infty) = \frac{1}{f_0}. \quad (18)$$

Similarly,

$$e_u(\infty) = B(\hat{\Delta}_u(\infty)f_0 - 1) = 0. \quad (19)$$

The expressions above show that time synchronization will eventually be achieved with an expected steady-state error of  $e_u(\infty) = 0$ .

In Appendix-(A), we show that the variance of this approach can be calculated as

$$\begin{aligned} Var(e(\infty)) &= \frac{\alpha \left( \frac{Bf_{max}^2}{3} + f_0^2 \sigma_d^2 \right)}{1 - \alpha \left( B^2 f_0^2 + \frac{Bf_{max}^2}{3} \right)} \left( B^2 + \frac{Bf_{max}^2}{3f_0^2} \right) \\ &\quad + \frac{Bf_{max}^2}{3f_0^2} + \sigma_d^2. \end{aligned} \quad (20)$$

It is apparent that as long as the inequality (16) is satisfied, the convergence will be established. However, the smaller the value of  $\alpha$ , the smaller the asymptotic variance. On the other hand, the convergence time is inversely related by the magnitude of the eigenvalue  $\lambda_2$  in equality (15). Hence, the smaller the  $\alpha$ , the bigger  $\lambda_2$  is and thus the longer the convergence time.

Figure (1) presents the evolution of the frequency of the logical clock of node  $u$  during a numerical simulation, from which we observe that the proposed synchronization approach establishes synchronization between two nodes and it is adaptive in terms of environmental dynamics, that fits perfectly for the wireless sensor networks.

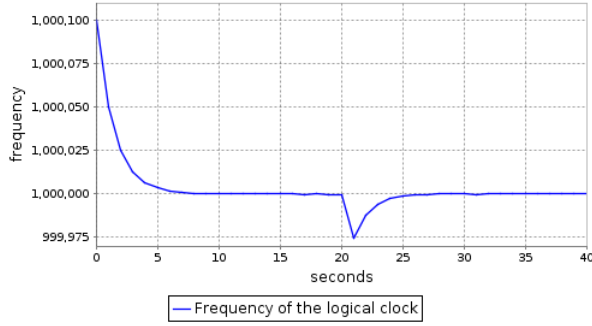


Figure 1. Simulation results related to  $f_u \hat{\Delta}_u$  during the synchronization between the reference node  $r$  and the node  $u$  with the following system parameters:  $B = 30$  seconds,  $f_0 = f_r = 1\text{MHz}$ ,  $f_{max} = 100\text{ppm}$  and  $\mathcal{T} \sim \mathcal{N}(0, \sigma_d^2 = 100\text{microseconds})$ . We set  $f_u - f_r = 100\text{ppm}$  and  $\alpha_u = 0.5$ . After a finite number of iterations, the logical clock frequency of node  $u$  converges to  $f_r$ . At iteration 20, the hardware clock frequency of node  $u$  is modified by setting  $f_u - f_r = 50\text{ppm}$ . In this case, the logical clock frequency of node  $u$  gets adapted and converges to  $f_r$  again.

#### D. Theoretical Comparison to PISync Algorithm

In Appendix-(B), we analyzed PI-Controller based PISync algorithm [8] under the same system model. Based on these results, we summarize the differences and similarities between GraDeS and PISync as follows:

- Since the largest eigenvector of the system matrix  $A$  of GraDeS is smaller than that of PISync, i.e.  $\lambda_2^{GraDeS} = 1 - 2\alpha B^2 f_0^2 < \lambda_2^{PISync} = 1 - 2\alpha B f_0$  when  $\alpha$  parameters are identical, time-to-convergence of GraDeS is superior than that of PISync.
- Considering asymptotic variances of GraDeS in equality (20) and that of PISync in equality (43), as long as the re-synchronization period satisfies  $B < \frac{1}{2f_0}$  and  $\alpha$  parameters are identical, the synchronization performance of GraDeS is superior than that of PISync. However, when practical parameters in Figure (1) are taken into account, such a synchronization period is not applicable which makes PISync a better choice, in theory.
- Since the update equations of GraDeS and PISync are quite similar, errors introduced by communication delays, quantization, etc., enter linearly to the system equations.<sup>1</sup>. Therefore, the synchronization errors of both approaches grow with the *square-root* of the network diameter, that gives rise to scalable synchronization performance degradation.

#### IV. MULTI-HOP SYNCHRONIZATION OF WSNS WITH GRADES

Algorithm (1) presents the pseudo-code for the Gradient Descent Synchronization (GraDeS) protocol that extends our pairwise synchronization scheme to multi-hop. For simplicity, it is assumed that the reference node  $r$  is predefined before the deployment of the sensor network. However, simple root election mechanisms (e.g. in [1]) can easily be integrated to the protocol. Whenever the hardware clock of any node reaches a multiple of  $B$  (Line 8), only the reference node increments

<sup>1</sup>Details are already given in [8]

---

#### Algorithm 1 GraDeS pseudo-code for node $u$ .

---

```

1: Upon receiving  $\langle l_v, seq_v \rangle$  such that  $seq_v > seq_u$ 
2:  $seq_u \leftarrow seq_v$ 
3:  $e_u \leftarrow l_u - l_v$ 
4:  $l_u \leftarrow l_v$ 
5: update  $\alpha_u$ 
6:  $\hat{\Delta}_u \leftarrow \hat{\Delta}_u - \alpha_u \nabla e_u$ 
7:
8: Upon  $h_u = kB$  where  $k \in \mathbb{N}$ 
9: if  $u = r$  then  $seq_u \leftarrow seq_u + 1$ 
10: broadcast  $\langle l_u, seq_u \rangle$ 

```

---

the sequence number (Line 9). Then, each node broadcasts a synchronization message that carries the value of its logical clock and its sequence number for their neighboring nodes in order to establish network-wide time synchronization (Line 10). It should be noted that  $l_r = h_r$  for the reference node and it does not participate in the synchronization process.

Sensor nodes other than the reference collect the synchronization messages that belong to the new synchronization round, i.e. with higher sequence numbers (Line 1). At the first step, they update their sequence number (Line 2) and calculate the synchronization error (Line 3). Then, they set their logical clock to the received time information for offset compensation (Line 4). Following this step, they update their step sizes (Line 5). We will explain the details of this step in the following paragraphs. Finally, they update their rate multipliers according to the gradient descent algorithm (Line 6). Observe that, in contrast to the regression table in least-squares, nodes executing GraDeS protocol do not require any memory to collect time information of the reference node. The operations during logical clock update (Lines 3-6) are quite simple and easy to implement as compared to the calculation of the least-squares line.

#### A. Adaptation of the Step Size

The step size  $\alpha$  has an important effect on both synchronization error performance and convergence time of the GraDeS algorithm. Choosing a constant and big step size would lead to a faster convergence but also a big steady state synchronization error. On the other hand, choosing a constant and small step size would lead to a slow convergence but smaller steady state synchronization error. When environmental dynamics in WSNS are considered, individual sensors should react to these changes fast and slow convergence would lead to a big problem. For this purpose, we modified the adaptation algorithm in [8], that adjusts step size adaptively in order to achieve fast convergence and small steady-state error, as shown below:

$$\alpha(t_h) = \begin{cases} 2\alpha(t_{h-1}) & \text{if } \nabla e(t_h) \cdot \nabla e(t_{h-1}) > 0 \\ 1/3\alpha(t_{h-1}) & \text{otherwise} \end{cases} \quad (21)$$

The intuition behind this approach is similar to that presented in [8]: Let  $t_h$  be the receipt time of a new synchronization message and let  $\nabla e(t_h)$  be the derivative of

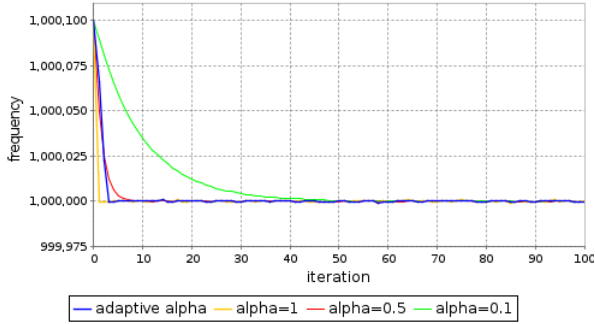


Figure 2. Simulation results related to the evolution of the logical clock frequency with different step sizes during the synchronization and between the reference node  $r$  and the node  $u$ . The parameter setting in Figure (1) were also used for these simulations. With constant step size, the convergence time increases but the steady state error decreases as the step size gets smaller. With adaptive algorithm, the convergence time is faster and the steady state error is quite comparable to those with constant step sizes.

the error observed at that time. If the derivative  $\nabla e(t_h)$  and the derivative of the previous round  $\nabla e(t_{h-1})$  have the same sign, i.e. their directions are the same, then the more  $\hat{\Delta}$  is supposed to be far away from its optimal value  $\hat{\Delta}^*$ . Hence, it necessary to *accelerate* the adjustment of  $\hat{\Delta}$  in order to reach  $\hat{\Delta}^*$  more quickly. On the contrary, if the signs of  $\nabla e(t_h)$  and  $\nabla e(t_{h-1})$  are opposite, then  $\hat{\Delta}$  is oscillating around  $\hat{\Delta}^*$ . In order to get closer to the optimal value, it is necessary to *decelerate* the adjustment. It is worth to mention that this algorithm is inspired from [4] in which the multipliers 2 and 1/3 are shown to be good values in terms of convergence performance. Figure (2) presents the evolution of the logical clock frequency of node  $u$  with constant and adaptive step sizes during a numerical simulation.<sup>2</sup>

## V. EXPERIMENTAL EVALUATION

We implemented GraDeS and PISync protocols for MICAz sensor platform using TinyOS 2.1.2 operating system. In order to evaluate their multi-hop synchronization performances, we prepared identical testbed setup as presented in [2], [3], [4] and preferred a line topology of 20 sensor nodes to evaluate scalability and adaptivity. We used 7.37 MHz quartz oscillator on the MICAz board as the clock source for the timer used for timing measurements. The timer operates at 1/8 of that frequency and thus each timer tick occurs at approximately every 921 kHz, i.e., approximately 1 microseconds, therefore,  $f_0 = 1$  MHz. During the experiments, each lasted approximately 20000 seconds, we fixed beacon period  $B = 30$  seconds and we collected instantaneous logical clock values from the nodes. For performance comparison, we considered *global skew* which is defined as the largest instantaneous clock difference between arbitrary nodes.

Performance evaluation of synchronization protocols in a fair manner is a challenging task since it is almost impossible to create identical message delays, packet loss rates and environmental conditions during tests that effect the frequency

<sup>2</sup>It should be noted that if  $\alpha(t_h) > \frac{1}{B^2 f_0^2}$  then  $\alpha(t_h) = \frac{1}{B^2 f_0^2}$  and if  $\alpha(t_h) = 0$  then  $\alpha(t_h) = \alpha(t_{h-1})$ .

of the crystal oscillators of the sensor nodes. To this end, we followed the same approach in [11] and we integrated both protocols to each sensor node since both GraDeS and PISync have identical message patterns. First, we enlarged the synchronization messages so that they carry the logical clock values calculated both using GraDeS and PISync. In this manner, when a synchronization message is received by a sensor node, it extracts the logical clock value for GraDeS and that for PISync to update its corresponding logical clocks. As a final modification, we added an interface to query the logical clock values calculated with GraDeS and PISync. With such modifications, we could evaluate both strategies under identical executions.

Figure (3) presents the synchronization performances of PISync and GraDeS. First, we observed that the convergence times of GraDeS and PISync were almost identical. Even though our theoretical comparison provided a slightly superior convergence time for GraDeS, this superiority was not observable in practice due to the practical values of the system parameters. Our second observation is the superiority of the synchronization performance of GraDeS over PISync at the time instants where there were error peaks after convergence is established, i.e. the peak around second 4300 and that around 14600. Apart from these points, the performances of both approaches were quite comparable. The reason for this phenomenon is related to the step size  $\alpha$  values. It is apparent that the step size boundaries of GraDeS, i.e.  $(0, \frac{1}{B^2 f_0^2}]$  is quite narrow than that of PISync, i.e.  $(0, \frac{2}{B f_0}]$ . This led to smaller step size values for GraDeS that allowed to be more robust against erroneous nodes. Moreover, step size adaptation of GraDeS is different than that of PISync, since in the former considers the sign of the derivative of the error whereas the latter considers the sign of the error. These differences led to a different reactive behavior. During the experiments, maximum global skew values after the convergence were 96 and 119 microseconds for GraDeS and PISync, respectively. However, neglecting peak points, their performances were quite identical.

For efficient duty-cycling of the radios, nodes should estimate when data is coming to switch on their radios for receiving the data. In particular, a *guard time* is necessary to compensate the synchronization errors. As indicated in [12], existing sleep/wake scheduling schemes assume that the underlying synchronization protocol can provide microsecond-level synchronization so that their guard times are small and nodes keep their radios on for a less amount of time, leading to less energy consumption. Therefore, the microsecond synchronization performance of GraDeS meets the typical requirements of the existing duty-cycling schemes and it can effectively be used by them. In our implementations, PISync and GraDeS had identical main memory overhead since they maintain three 32 bit variables  $\hat{t}_u(t_{up})$ ,  $\hat{\Delta}_u(t_{up})$  and  $h_u(t_{up})$  for logical clock, and additional 32 bits are required for the step size adaptation. Since these protocols have identical communication frequencies, their energy consumption during a packet processing and updating

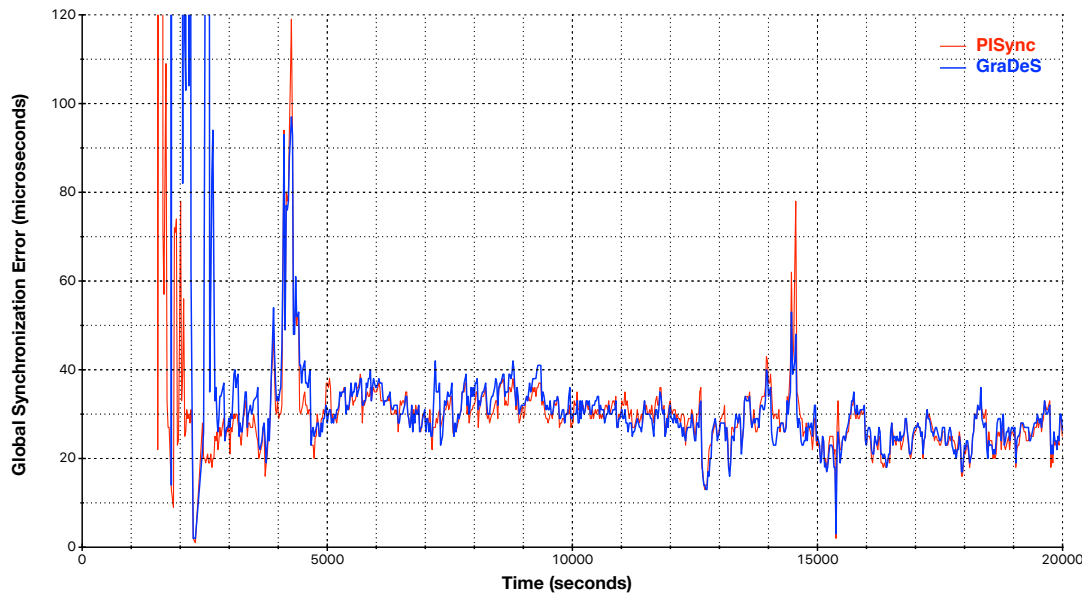


Figure 3. Instantaneous and average global synchronization errors for GraDeS and PISync.

the logical clock are quite comparable. We refer the reader [13] for a detailed discussion of these issues.

## VI. CONCLUSION AND FUTURE WORK

In this article, we formulated pairwise synchronization process as an optimization problem and showed that it can efficiently be solved by employing gradient descent algorithm. We introduced a new time synchronization protocol, namely *Gradient Descent Synchronization (GraDeS)*, that establishes multi-hop synchronization based upon this algorithm. We gave details about our implementation and presented the experimental evaluation on our testbed of MICAz sensor nodes. A future research direction can be the integration of the proposed approach to duty-cycling MAC protocols in WSNs in order to observe its impact on the conservation of the energy. Another point worth to explore is to integrate GraDeS to real-world applications to evaluate its actual performance.

## REFERENCES

- [1] M. Maróti, B. Kusy, G. Simon, and A. Lédeczi, "The flooding time synchronization protocol," in *Proceedings of the 2Nd International Conference on Embedded Networked Sensor Systems*, ser. SenSys '04. New York, NY, USA: ACM, 2004, pp. 39–49. [Online]. Available: <http://doi.acm.org/10.1145/1031495.1031501>
- [2] C. Lenzen, P. Sommer, and R. Wattenhofer, "Pulsesync: An efficient and scalable clock synchronization protocol," *Networking, IEEE/ACM Transactions on*, vol. PP, no. 99, pp. 1–1, 2014.
- [3] K. Yildirim and A. Kantarci, "Time synchronization based on slow-flooding in wireless sensor networks," *Parallel and Distributed Systems, IEEE Transactions on*, vol. 25, no. 1, pp. 244–253, 2014.
- [4] K. S. Yildirim and Ö. Gürçan, "Efficient time synchronization in a wireless sensor network by adaptive value tracking," *Wireless Communications, IEEE Transactions on*, vol. PP, no. 99, pp. 1–1, 2014.
- [5] M. Leng and Y.-C. Wu, "Low-complexity maximum-likelihood estimator for clock synchronization of wireless sensor nodes under exponential delays," *Signal Processing, IEEE Transactions on*, vol. 59, no. 10, pp. 4860–4870, 2011.
- [6] —, "Distributed clock synchronization for wireless sensor networks using belief propagation," *Signal Processing, IEEE Transactions on*, vol. 59, no. 11, pp. 5404–5414, Nov 2011.
- [7] J.-M. Berthaud, "Time synchronization over networks using convex closures," *IEEE/ACM Trans. Netw.*, vol. 8, no. 2, pp. 265–277, Apr. 2000. [Online]. Available: <http://dx.doi.org/10.1109/90.842147>
- [8] K. S. Yildirim, R. Carli, and L. Schenato, "Adaptive control-based clock synchronization in wireless sensor networks," in *European Control Conference ECC15*, ser. ECC'15, 2015.
- [9] S. Boyd and L. Vandenberghe, *Convex Optimization*. New York, NY, USA: Cambridge University Press, 2004.
- [10] H. Huang, J. Yun, Z. Zhong, S. Kim, and T. He, "Psr: Practical synchronous rendezvous in low-duty-cycle wireless networks," in *INFOCOM, 2013 Proceedings IEEE*, 2013, pp. 2661–2669.
- [11] K. S. Yildirim and A. Kantarci, "Drift estimation using pairwise slope with minimum variance in wireless sensor networks," *Ad Hoc Netw.*, vol. 11, no. 3, pp. 765–777, May 2013.
- [12] Y. Wu, S. Fahmy, and N. B. Shroff, "Optimal sleep/wake scheduling for time-synchronized sensor networks with qos guarantees," *IEEE/ACM Trans. Netw.*, vol. 17, no. 5, pp. 1508–1521, Oct. 2009. [Online]. Available: <http://dx.doi.org/10.1109/TNET.2008.2010450>
- [13] K. S. Yildirim, R. Carli, and L. Schenato, "Proportional-integral clock synchronization in wireless sensor networks," *CoRR*, vol. abs/1410.8176, 2014. [Online]. Available: <http://arxiv.org/abs/1410.8176>



**Kasım Sinan Yildirim** received the BSc(Eng), M.Sc. and Ph.D. degrees from Department of Computer Engineering, Ege University, Izmir, Turkey in 2003, 2006 and 2012 respectively. He worked as a research assistant between 2007-2013 and as an assistant professor between 2013-2015 at the same department. Currently, he is a postdoctoral researcher at Embedded Software Group, TU Delft, The Netherlands. His research interests are embedded systems, distributed systems, distributed algorithms, wireless sensor networks, wireless power transfer networks and computational RFIDs. He is a member of IEEE.

APPENDIX A  
ASYMPTOTIC VARIANCE OF GRADES

Define  $w_{h+1} = \int_{t_h}^{t_{h+1}} u(t)dt$ . Applying straightforward steps,  $\int_{h+}^{t_{h+1}} f(t)dt$  becomes:

$$\begin{aligned} \int_{h+}^{t_{h+1}} f(t)dt &= \int_{h+}^{t_{h+1}} (f_0 + u(t)) dt \\ &= Bf_0 + \int_{t_h}^{t_{h+1}} u(t)dt \\ &= Bf_0 + w_{h+1} \end{aligned} \quad (22)$$

From the definition of  $w_{h+1}$  and the properties of the uniform random variables, it holds that  $E[w_{h+1}] = 0$  and  $E[w_{h+1}^2] = \frac{Bf_{max}^2}{3}$ . Now, define  $z_h = \hat{\Delta}(h)f_0 - 1$  and  $d_{h+1} = \mathcal{T}_{h+1} - \mathcal{T}_h$ . With these definitions, the error function can be written as:

$$\begin{aligned} e(h+1) &= \hat{\Delta}(h) \int_{h+}^{h+1} f(t)dt - (B + \mathcal{T}_{h+1} - \mathcal{T}_h) \\ &= Bz_h + \hat{\Delta}(h)w_{h+1} - d_{h+1} \\ &= Bz_h + \left(\frac{z_h + 1}{f_0}\right)w_{h+1} - d_{h+1} \\ &= z_h \left(B + \frac{w_{h+1}}{f_0}\right) + \frac{w_{h+1}}{f_0} - d_{h+1}. \end{aligned} \quad (23)$$

Similarly, for  $\hat{\Delta}(h+1)$  we can apply the following steps:

$$\begin{aligned} \hat{\Delta}(h+1) &= \hat{\Delta}(h) - 2\alpha Bf_0 e(h+1) \\ &= \frac{z_h + 1}{f_0} \\ &\quad - 2\alpha Bf_0 \left( z_h \left( B + \frac{w_{h+1}}{f_0} \right) + \frac{w_{h+1}}{f_0} - d_{h+1} \right) \\ &= z_h \left( \frac{1}{f_0} - 2\alpha Bf_0 \left( B + \frac{w_{h+1}}{f_0} \right) \right) \\ &\quad + \frac{1}{f_0} - 2\alpha Bf_0 \left( \frac{w_{h+1}}{f_0} - d_{h+1} \right). \end{aligned} \quad (24)$$

Let  $g_{h+1} = Bf_0 + w_{h+1}$ . Then,  $z_{h+1} = \hat{\Delta}(h+1)f_0 - 1$  becomes:

$$\begin{aligned} z_{h+1} &= z_h (1 - 2\alpha Bf_0 g_{h+1}) - 2\alpha Bf_0 g_{h+1} \\ &\quad + 2\alpha Bf_0^2 (B + d_{h+1}). \end{aligned} \quad (25)$$

It easy to see that  $z_h$ ,  $g_{h+1}$  and  $d_{h+1}$  are independent random variables. Similarly, we have  $E[g_{h+1}] = Bf_0$  and  $E[g_{h+1}^2] = B^2 f_0^2 + \frac{Bf_{max}^2}{3}$ . Therefore:

$$E[z_{h+1}] = E[z_h] (1 - 2\alpha B^2 f_0^2). \quad (26)$$

that clearly shows that

$$\lim_{h \rightarrow \infty} E[z_h] = 0. \quad (27)$$

Similarly, after some calculations, we can obtain:

$$\lim_{h \rightarrow \infty} E[z_h^2] = \frac{\alpha \left( \frac{Bf_{max}^2}{3} + f_0^2 \sigma_d^2 \right)}{1 - \alpha \left( B^2 f_0^2 + \frac{Bf_{max}^2}{3} \right)}.$$

Now, let us bring our attention to the asymptotic variance of the error function. Considering equation (23), it holds that

$$\lim_{h \rightarrow \infty} E[e(h+1)] = BE[z_h] = 0. \quad (28)$$

and

$$\begin{aligned} \lim_{h \rightarrow \infty} E[(e(h+1))^2] &= E[z_h^2] \left( B^2 + \frac{E[w_{h+1}^2]}{f_0^2} \right) \\ &\quad + \frac{E[w_{h+1}^2]}{f_0^2} + E[d_{h+1}^2] \\ &= \frac{\alpha \left( \frac{Bf_{max}^2}{3} + f_0^2 \sigma_d^2 \right)}{1 - \alpha \left( B^2 f_0^2 + \frac{Bf_{max}^2}{3} \right)} \left( B^2 + \frac{Bf_{max}^2}{3f_0^2} \right) \\ &\quad + \frac{Bf_{max}^2}{3f_0^2} + \sigma_d^2. \end{aligned} \quad (29)$$

Finally, the asymptotic error variance can be obtained as follows:

$$\begin{aligned} \lim_{h \rightarrow \infty} \text{Var}(e(h+1)) &= E[(e(h+1))^2] - (E[e(h+1)])^2 \\ &= E[(e(h+1))^2]. \end{aligned} \quad (30)$$

APPENDIX B  
THEORETICAL COMPARISON TO PISYNC

In [8], the update equations of the PI controller based time synchronization protocol PISync is given as:

$$l_u(t_h^+) = t_h + \mathcal{T}_h, \quad (31)$$

$$\hat{\Delta}_u(t_h^+) = \hat{\Delta}_u(t_h) - \alpha e_u(t_h). \quad (32)$$

Therefore, the update equations of PISync algorithm can be described with the following matrix equation:

$$\underbrace{\begin{bmatrix} e(h+1) \\ \hat{\Delta}_u(h+1) \end{bmatrix}}_{X(h+1)} = \begin{bmatrix} 0 & \int_{t_h}^{t_{h+1}} f_u(t)dt \\ 0 & 1 - \alpha \int_{t_h}^{t_{h+1}} f_u(t)dt \end{bmatrix} \underbrace{\begin{bmatrix} e(h) \\ \hat{\Delta}_u(h) \end{bmatrix}}_{X(h)} + (B + \mathcal{T}_{h+1} - \mathcal{T}_h) \begin{bmatrix} -1 \\ \alpha \end{bmatrix}. \quad (33)$$

Taking the expectation of both sides yields

$$E[X(h+1)] = \underbrace{\begin{bmatrix} 0 & Bf_0 \\ 0 & 1 - \alpha Bf_0 \end{bmatrix}}_A E[X(h)] + \begin{bmatrix} -B \\ \alpha B \end{bmatrix}. \quad (34)$$

and the eigenvalues of the matrix  $A$  can be obtained as:

$$\lambda_1 = 0, \lambda_2 = 1 - \alpha B f_0. \quad (35)$$

Consequently, asymptotic convergence is established, if and only if

$$0 < \alpha < \frac{2}{B f_0}. \quad (36)$$

Finally, we get for  $\hat{\Delta}_u(\infty)$  and  $e_u(\infty)$  that

$$\hat{\Delta}_u(\infty) = (1 - \alpha B f_0) \hat{\Delta}_u(\infty) + \alpha B = \frac{1}{f_0}, \quad (37)$$

$$e_u(\infty) = B(\hat{\Delta}_u(\infty) f_0 - 1) = 0. \quad (38)$$

#### A. Asymptotic Variance

Following the steps in Appendix-(A),  $\hat{\Delta}(h+1)$  can be written as:

$$\begin{aligned} \hat{\Delta}(h+1) &= \hat{\Delta}(h) - \alpha e(h+1) \\ &= \frac{z_h + 1}{f_0} - \alpha \left( z_h \left( B + \frac{w_{h+1}}{f_0} \right) + \frac{w_{h+1}}{f_0} - d_{h+1} \right) \\ &= z_h \left( \frac{1}{f_0} - \alpha \left( B + \frac{w_{h+1}}{f_0} \right) \right) + \frac{1}{f_0} \\ &\quad - \alpha \left( \frac{w_{h+1}}{f_0} - d_{h+1} \right). \end{aligned} \quad (39)$$

Then,  $z_{h+1} = \hat{\Delta}(h+1) f_0 - 1$  becomes:

$$z_{h+1} = z_h (1 - \alpha g_{h+1}) - \alpha g_{h+1} + \alpha f_0 (B + d_{h+1}). \quad (40)$$

After some straightforward steps, we obtain the asymptotic value of  $E[z_h]$  as

$$\lim_{h \rightarrow \infty} E[z_h] = 0 \quad (41)$$

and the asymptotic value of  $E[z_h^2]$  as

$$\lim_{h \rightarrow \infty} E[z_h^2] = \frac{\alpha \left( \frac{B f_{max}^2}{3} + f_0^2 \sigma_d^2 \right)}{2B f_0 - \alpha \left( B^2 f_0^2 + \frac{B f_{max}^2}{3} \right)}. \quad (42)$$

Finally, we calculate mean squared-error, which is also the asymptotic variance as:

$$\begin{aligned} E[(e(h+1))^2] &= E[z_h^2] \left( B^2 + \frac{E[w_{h+1}^2]}{f_0^2} \right) \\ &= + \frac{E[w_{h+1}^2]}{f_0^2} + E[d_{h+1}^2] \\ &= \frac{\alpha \left( \frac{B f_{max}^2}{3} + f_0^2 \sigma_d^2 \right)}{2B f_0 - \alpha \left( B^2 f_0^2 + \frac{B f_{max}^2}{3} \right)} \left( B^2 + \frac{B f_{max}^2}{3 f_0^2} \right) \\ &\quad + \frac{B f_{max}^2}{3 f_0^2} + \sigma_d^2. \end{aligned} \quad (43)$$